Symmetry-breaking and symmetry-restoring dynamics of a mixture of Bose-Einstein condensates in a double well

Indubala I. Satija,[1,2] Radha Balakrishnan,[3] Phillip Naudus,[1] Jeffrey Heward,[4] Mark Edwards,[4,2] and Charles W. Clark[2]
[1]*Department of Physics, George Mason University, Fairfax, Virginia 22030, USA*
[2]*National Institute of Standards and Technology, Gaithersburg, Maryland 20899, USA*
[3]*The Institute of Mathematical Sciences, Chennai 600 113, India*
[4]*Department of Physics, Georgia Southern University, Statesboro, Georgia 30460-8031, USA*
(Received 12 November 2008; published 16 March 2009)

We study the coherent nonlinear tunneling dynamics of a binary mixture of Bose-Einstein condensates in a double-well potential. We demonstrate the existence of a type of mode associated with the "swapping" of the two species in the two wells of the potential. In contrast to the *symmetry-breaking* macroscopic quantum self-trapping (MQST) solutions, the swapping modes correspond to the tunneling dynamics that preserves the symmetry of the double-well potential. As a consequence of two distinct types of broken-symmetry MQST phases where the two species localize in different potential wells or coexist in the same well, the corresponding symmetry-restoring swapping modes result in dynamics where the two species either avoid or chase each other. In view of the possibility to control the interaction between the species, the binary mixture offers a very robust system to observe these novel effects as well as the phenomena of Josephson oscillations and π modes.

DOI: 10.1103/PhysRevA.79.033616 PACS number(s): 03.75.Mn, 34.50.−s

I. INTRODUCTION

Ultracold laboratories have had great success in creating Bose-Einstein condensates (BECs) [1] in a variety of atomic gases such as rubidium (Rb), lithium (Li), sodium (Na), and ytterbium (Yb). These quantum fluids exist in various isotopic forms as well as in different hyperfine states. The rapid pace of development in this field has led to condensates which are robust and relatively easy to manipulate experimentally. In particular, the tunability of interspecies and intraspecies interactions [2] via magnetic and optical Feshbach resonances makes the BEC mixture a very attractive candidate for exploring new phenomena involving quantum coherence and nonlinearity in a multicomponent system.

The subject of this paper is to investigate the tunneling dynamics of a binary mixture of BECs in a double-well potential. A single species of BEC in a double well is called a bosonic Josephson junction (BJJ), since it is a bosonic analog of the well-known superconducting Josephson junction. In addition to Josephson oscillations (JO), the BJJ exhibits various novel phenomena such as π modes and macroscopic quantum self-trapping (MQST), as predicted theoretically [3,4]. In the JO and the π modes, the condensate oscillates symmetrically about the two wells of the potential. In contrast to this, the MQST dynamics represents a broken-symmetry phase as the tunneling solutions exhibit population imbalance between the two wells of the potential. These various features have been observed experimentally [5]. Our motivation is to explore whether new phenomena arise when there are two interacting condensates trapped in a symmetric double well.

Although our formulation and results are valid for a variety of BEC mixtures, our main focus here is the Rb family of two isotopes, namely, the mixture of ^{87}Rb and ^{85}Rb, motivated by the experimental setup at JILA [6]. The scattering length of ^{87}Rb is known to be 100 a.u. while the interspecies scattering length is 213 a.u. In experiments, the scattering length of ^{85}Rb can be tuned using the Feshbach resonance method [7].

The ability to tune the scattering length of one of the species makes this mixture of isotopes an ideal candidate for studying the coupled BJJ system. First, it opens up the possibility of exploring the parameter space where the ^{85}Rb-^{85}Rb scattering length is equal to the ^{87}Rb-^{87}Rb scattering length. As will be discussed below, this symmetric parameter regime simplifies the theoretical analysis of the system and also captures most of the new phenomena that underlie the dynamics of the binary mixture. Furthermore, the tunability of the ^{85}Rb scattering length can be exploited to study a unique possibility where one of the species has a negative scattering length, a case which strongly favors the π-mode oscillations that have not been observed so far.

In our exploration of nonlinear tunneling dynamics of coupled BJJ systems, the MQST states are found to be of two types. In the broken-symmetry MQST state, the two components may localize in different wells resulting in a phase separation or they may localize in the same well and hence coexist. By varying the parameters such as initial conditions, the phase-separated broken-symmetry MQST states can be transformed to a symmetry-restoring phase where the species continually "avoid" each other by swapping places between the two wells. In other words, if the dynamics is initiated with both species in the same potential well, the sustained tunneling oscillations are seen where the two species swap places between the well one and the well two. From the coexisting MQST phase, one can achieve symmetry restoring swapping dynamics by initiating the dynamics with two species in the separate wells. In this case, the emergence of the swapping modes can be interpreted as a phase where the two species "chase" each other.

The paper is organized as follows. In Sec. II, we discuss the model and use the two-mode approximation to the Gross–Pitaevskii (GP) equation to map it to a system of two coupled pendulums with momentum-dependent lengths and

coupling. Section III discusses the stationary solutions and Section IV discusses their stability. These results enable us to look for various qualitatively different effects without actually solving the GP equations. Section V describes the numerical solutions of the GP equations as various parameters of the system are tuned. Although we have explored the multidimensional parameter space, the novelties attributed to the binary mixture in a double-well trap are presented in a restricted parameter space where the scattering lengths of the two species are equal. Additionally, in our numerical results described here, we fix the ratio of ^{87}Rb-^{87}Rb interaction to ^{85}Rb-^{87}Rb interaction to be 2.13. This restricted parameter space is accessible in the JILA setup and provides a simple means to describe various highlights of the mixture dynamics. Section VI provides additional details of the JILA setup relevant for our investigation. A summary is given in Sec. VII.

II. TWO-MODE GP EQUATION FOR THE BINARY MIXTURE

In the semiclassical regime where the fluctuations around the mean values are small, the two-component BEC is described by the following coupled GP equations for the two condensate wave functions $\Phi_l(x,t)$, with $l=a,b$ representing the two species in the mixture:

$$i\hbar\dot{\Phi}_a = \left(-\frac{\hbar^2}{2m_a}\nabla^2 + V_a\right)\Phi_a + (g_a|\Phi_a|^2 + g_{ab}|\Phi_b|^2)\Phi_a,$$

$$i\hbar\dot{\Phi}_b = \left(-\frac{\hbar^2}{2m_b}\nabla^2 + V_b\right)\Phi_b + (g_b|\Phi_b|^2 + g_{ab}|\Phi_a|^2)\Phi_b.$$

Here, m_l, V_l, and $g_l=4\pi\hbar^2 a_l/m_l$ denote, respectively, the mass, the trapping potential, and the intra-atomic interaction of each species, with a_l as the corresponding scattering length. $g_{ab}=2\pi\hbar^2(1/m_a+1/m_b)a_{ab}$ is the interspecies interaction, where a_{ab} is the corresponding scattering length. For the JILA experiment, in view of the tight confinement of the condensate transverse to the trap, it is sufficient to consider the corresponding one-dimensional Gross-Pitaevskii equations (GPE).

The condensate wave functions satisfy the normalization conditions

$$\int d^3r|\Phi_l|^2 = N_l. \tag{1}$$

The total number of atoms in the mixture is $N=N_a+N_b$.

Previous studies have investigated the stability of binary BEC mixture characterized by three different scattering lengths [8] and have pointed out the possibility that the coupling parameters may depend upon each other. Our studies investigating the tunneling dynamics of the BEC mixture in a double well will focus on robust behavior that exists in a wide range of parameters and initial conditions and should be observable in experiments that typically have multiple knobs that tune the parameters.

In the weakly linked limit, the dynamical oscillations of the two-component BEC can be described by two wave functions representing the condensate in each trap labeled by $k=1,2$, with the spatial and the temporal contributions factored as follows [3,9–11]:

$$\begin{pmatrix}\Phi_a\\ \Phi_b\end{pmatrix} = \begin{pmatrix}\chi_1^a(x)\psi_1^a(t)\\ \chi_1^b(x)\psi_1^b(t)\end{pmatrix} + \begin{pmatrix}\chi_2^a(x)\psi_2^a(t)\\ \chi_2^b(x)\psi_2^b(t)\end{pmatrix} \tag{2}$$

The localized spatial modes $\chi_k^{(l)}(x)$ are computed as sums and differences of the symmetric and antisymmetric solutions of the time-independent coupled GP equations [3,9]. To derive the equations of motion in the two-mode approximation, we introduce $z_l(t)$, the population imbalance, and $\phi_l(t)$, the relative phase of species l between the left and right sides of the double-well potential,

$$z_l(t) = (|\psi_1^l|^2 - |\psi_2^l|^2)/N, \tag{3}$$

$$\phi_l(t) = (\theta_1^l - \theta_2^l), \tag{4}$$

where $\psi_k^{(l)}(t)=|\psi_k^{(l)}(t)|\exp i\theta_k^{(l)}$ are the time-dependent coefficients in the two-mode equations.

Following the methodology of previous works related to single-component BEC [3,9] we substitute Eq. (2) into the coupled GP equations. Using the orthogonality and the definite parity of the spatial modes, we integrate out the spatial degrees of freedom [9]. We would like to emphasize that we follow the so-called "improved-two-mode" approach [9] where we retain *all overlap integrals*. In the case of single species, this has been shown to be an improvement over the previous approach [3] where the overlap integrals involving the spatial modes χ_1 and χ_2 were neglected. In other words, given the ansatz (2), we average over the spatial part from the coupled partial differential equations (coupled GPE), resulting in coupled ordinary differential equations. The spatial averaging leads to the renormalization of the bare coupling parameters g_i.

The four coupled nonlinear ordinary differential equations which we refer to as the "two-mode" model are

$$\dot{Z}_a = -\bar{K}_a\sqrt{1-Z_a^2}\sin\phi_a, \tag{5}$$

$$\dot{Z}_b = -\bar{K}_b\sqrt{1-Z_b^2}\sin\phi_b, \tag{6}$$

$$\dot{\phi}_a = \bar{\Lambda}_a Z_a + \Lambda_{ab}Z_b + \bar{K}_a\frac{Z_a}{\sqrt{1-Z_a^2}}\cos\phi_a, \tag{7}$$

$$\dot{\phi}_b = \bar{\Lambda}_b Z_b + \Lambda_{ab}Z_a + \bar{K}_b\frac{Z_b}{\sqrt{1-Z_b^2}}\cos\phi_b, \tag{8}$$

where $Z_l=z_l/f_l$. In the above equations, $f_l=N_l/N$ denotes the fraction of atoms of species l, while the renormalized parameters $\bar{K}_l$ and $\bar{\Lambda}_l$ are given by

$$\bar{K}_a = K_a - 2f_aC_a\sqrt{1-Z_a^2}\cos\phi_a + f_bD_{ab}\sqrt{1-Z_b^2}\cos\phi_b,$$

$$\bar{K}_b = K_b - 2f_bC_b\sqrt{1-Z_b^2}\cos\phi_b + f_aD_{ba}\sqrt{1-Z_a^2}\cos\phi_a,$$

$$\bar{\Lambda}_a = \Lambda_a + C_a,$$

$$\bar{\Lambda}_b = \Lambda_b + C_b.$$

In the above, the space and time-independent parameters K_l, Λ_l, Λ_{ab}, C_l, and D_{ab} can be expressed in terms of various microscopic parameters that appear in GP equation and the localized modes, $\chi_k^l(x)$, and their overlap (integrated over spatial degrees of freedom). The explicit expressions for these parameters are given in the Appendix.

The parameters K_l describe the tunneling amplitude while Λ_l is related to the corresponding scattering length of the species. The parameters C_l and D_{ab} have their origin in the overlaps between the spatial modes χ_1 and χ_2 and are expected to be small in the weak tunneling limit. These overlaps modify the bare parameters denoted by the interaction Λ_l and the tunneling K_l. Consequently, we have a variable tunneling model, since the tunneling parameters $\bar{K}_l$ depend explicitly on the dynamical variables Z_l and ϕ_l.

It should be noted that the coupled Eqs. (5)–(8) and the relationship between the bare and the renormalized tunneling amplitudes as given below Eqs. (5)–(8) reveal a simple pattern suggesting straightforward generalization to more than two-component systems. In our analysis, we will mostly restrict ourselves to the case where the two species are equally populated, namely, $f_a = f_b = 1/2$. In this case, the above system of Eq. (8) can be viewed as the Hamiltonian equation in terms of the canonical variables Z_l (momenta) and ϕ_l (coordinates), with the Hamiltonian given by the following form:

$$H = \frac{1}{2}[\bar{\Lambda}_a Z_a^2 + \bar{\Lambda}_b Z_b^2 + 2\Lambda_{ab} Z_a Z_b] - \sum_{l=a,b} \bar{K}_l \sqrt{1 - Z_l^2} \cos \phi_l. \tag{9}$$

For the case where the overlap between the spatial modes χ_1 and χ_2 can be neglected and the effective tunneling $\bar{K}_l$ can be replaced by its bare value K_l, the above system can be viewed as a coupled pair of nonrigid pendulums, with momentum-dependent lengths. The coupling between the pendulums is also momentum dependent.

We parenthetically remark that this system can also be mapped to a pair of classical spins with Cartesian components

$$S_x^l = \sqrt{1 - Z_l^2} \cos \phi_l,$$

$$S_y^l = \sqrt{1 - Z_l^2} \sin \theta_l,$$

$$S_z^l = Z_l,$$

so that $(S^l)^2 = 1$. Thus the spin vector locates a point on the unit sphere given by polar angles θ_l, ϕ_l, with $Z_l = \cos \theta_l$. The corresponding spin Hamiltonian, written in terms of bare variables, can be shown to be

$$H = \sum_{l=a,b} \left[\frac{1}{2}(\Lambda_l + C_l)(S_z^l)^2 + C_l (S_x^l)^2 - K_l S_x^l \right] + \Lambda_{ab}(S_z^a S_z^b) - D_{ab}(S_x^a S_x^b).$$

The spin mapping provides an alternative means to visualize the effective interaction between the two species during the tunneling. If we ignore the spatial overlap integrals between the localized modes in two wells, $(C_l = 0, D_{ab} = 0)$, the binary mixture of condensates in two-mode approximation maps to two Ising-type spins in a transverse magnetic field. The full two-mode variable tunneling feature induces *XY*-like spin interaction.

In this paper, we find it convenient to exploit mapping to the coupled pendulums for exploring tunneling dynamics in the coupled BJJ. Although we have explored the full two-mode variable tunneling model, we will only discuss the constant tunneling case ($\bar{K}_l$ replaced by K_l and $\bar{\Lambda}_l$ replaced by Λ_l) as the overlap integrals are small and the various novel effects of the mixture described here are found to be robust and unaffected by the variable tunneling parameters.

III. STATIONARY SOLUTIONS: FIXED POINTS

The solutions of the coupled system are characterized by the interactions Λ_l, the ratio of the tunneling amplitude for the two species, K_a/K_b which we denote by R as well as the initial phase difference $\phi_l(t=0)$, and the initial population imbalance $Z_l(t=0)$. In the multidimensional parameter space the equilibrium or fixed-point solutions, in which the right-hand-sides of Eq. (8) are zero, provide an effective tool to classify different categories of behavior of the system.

In general, these fixed-point equations are transcendental and have to be solved numerically. However, in the symmetric case where $\Lambda_a = \Lambda_b = \Lambda$, $K_a = K_b = K$, the fixed-point equations can be tackled analytically. Further, as can be seen from Eq. (8), the parameter K can be eliminated in this case by rescaling $t(t \to Kt)$ and redefining Λ_x as $\Lambda_x \to \Lambda_x/K$. Our detailed analysis shows that this special case captures many relevant phenomena characterizing the binary mixture in a double well. In this case, the fixed points belong to two broad categories as stated below, resulting in two types of small amplitude oscillations about these two fixed points:

(i) Zero-mode fixed points $(\phi_a^* = \phi_b^* = 0)$,

(1) $Z_a^* = Z_b^* = 0$,

(2) $Z_a^* = -Z_b^* = \pm \frac{\sqrt{(\Lambda_{ab} - \Lambda)^2 - 4K^2)}}{|(\Lambda_{ab} - \Lambda)|}$.

(ii) π-mode fixed points $(\phi_a^* = \phi_b^* = \pi)$,

(1) $Z_a^* = Z_b^* = 0$,

(2) $Z_a^* = Z_b^* = \pm \frac{\sqrt{(\Lambda_{ab} + \Lambda)^2 - 4K^2)}}{|(\Lambda_{ab} + \Lambda)|}$.

It should be noted that the mixed-mode fixed points, $\phi_a^* = 0$ and $\phi_b^* = \pi$, $Z_a^* = Z_b^* = 0$, are unstable for the restricted parameter regime we are considering here and hence will not be discussed.

The small oscillations about the fixed-point $(Z^* = 0, \phi^* = 0)$ result in zero mode while small oscillations about $(Z^* = 0, \phi^* = \pi)$ lead to π mode. The oscillation frequencies are in Sec. IV.

The nontrivial fixed points $(Z^* \neq 0)$ result in solutions with population imbalance and lead to tunneling dynamics with macroscopic quantum self-trapping or the MQST. In view of the *a*-*b* symmetry, we have two sets of stationary solutions: Z_x^* and $-Z_x^*$), $(x = a, b)$. This suggests the possibility of modes where each species oscillates about the binary fixed

points, going back and forth between the two wells. Unlike MQST, these modes will preserve the symmetry of the double well. However, in contrast to zero modes, these modes are nonlinear and give rise to "swapping phase" that will be discussed later.

The emergence of fixed points with opposite signs for the two species ($Z_a^*=-Z_b^*$) in the zero mode phase suggests that MQST in zero mode is accompanied by phase separation of the two species. In contrast, in the π-mode MQST phase, the two species could coexist in the same potential well as ($Z_a^*=Z_b^*$). Therefore, the fixed-point equations suggest that π modes mimic attractive interaction between the two species.

The onset from oscillatory to MQST phase corresponds to the values of the parameters where the nontrivial fixed points move from the complex to the real plane. Alternatively, the condition for the broken-symmetry phase can be obtained by linear stability analysis of the fixed-point equations. This is discussed in Sec. IV.

In the asymmetric case when $\Lambda_a \neq \Lambda_b$ the fixed points are obtained by solving the coupled transcendental equations

$$(-1)^p \frac{K_a Z_a^*}{\sqrt{1-(Z_a^*)^2}} + \frac{1}{2}(\Lambda Z_a^* + \Lambda_{ab} Z_b^*) = 0,$$

$$(-1)^p \frac{K_b Z_b^*}{\sqrt{[1-(Z_b^*)^2]}} + \frac{1}{2}(\Lambda Z_b^* + \Lambda_{ab} Z_a^*) = 0,$$

where $p=0(1)$ for $\phi_a^*=0(\pi)$ and $\phi_b^*=0(\pi)$. Analogous to the symmetric case, both the zero and the π-mode solutions including those corresponding to MQST can be found numerically. As expected, for the MQST fixed points $Z_a^* \neq -Z_b^*$ in the zero mode and $Z_a^* \neq Z_b^*$ in the π mode and we do not have the permutation symmetry or the a-b symmetry. However, unlike the symmetric case, K_i's do not scale time t and the parameters and hence the ratio $R=\frac{K_a}{K_b}$ emerge as a new parameter.

IV. NORMAL MODES: LINEAR STABILITY ANALYSIS OF FIXED POINTS

Frequencies of small amplitude oscillations about $(Z^*=0, \phi^*=0)$ and $(Z^*=0, \phi^*=\pi)$, respectively, referred to as the zero mode or the π modes, are given by

$$\omega^2 = \frac{1}{2}(K_a\Lambda_a^* + K_b\Lambda_b^*) + \frac{1}{2} \pm \sqrt{(K_a\Lambda_a^* - K_b\Lambda_b^*)^2 + 4K_aK_b\Lambda_{ab}^2}],$$

where

$$\Lambda_a^* = (-1)^p K_a + \Lambda_a,$$

$$\Lambda_b^* = (-1)^p K_b + \Lambda_b,$$

where $p=0$ for the zero mode and $p=1$ for the π mode. In the symmetric case, with $\Lambda_a=\Lambda_b$ and $f_a=f_b$, the normal-mode frequencies ω_0 and ω_π simplify to

$$\omega_0^2 = K^2 + K(\Lambda \pm \Lambda_{ab})/2,$$

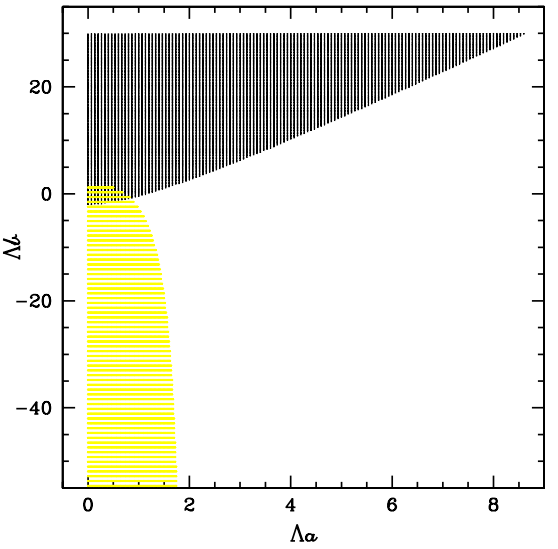

FIG. 1. (Color online) The upper (black) and the lower (yellow) shaded regime corresponds to the parameter values for the existence of stable zero mode and π mode with $R=K_a/K_b=1$.

$$\omega_\pi^2 = K^2 - K(\Lambda \pm \Lambda_{ab})/2.$$

The condition for the instability of the fixed point is determined when one of the normal-mode frequencies becomes complex. This gives rise to new fixed points where $Z_x^* \neq 0$ resulting in MQST phase where there is a population imbalance between the two wells of the double-well potential for each species. The condition for the existence of MQST is given by

$$f_a f_b \Lambda_{ab}^2 \geq \Lambda_a^* \Lambda_b^*. \tag{10}$$

In the zero-mode case, this inequality gives the condition for phase separation (see Sec. V C for further details) of the two species as $Z_a^*=-Z_b^*$. It should be noted that in the weak tunneling limit when $K_i < \Lambda_i$, the above equation is reminiscent of the phase-separation condition, $g_{ab}^2 \geq g_a g_b$, obtained using Thomas-Fermi approximation. Our analysis is in fact valid only in the weak tunneling limit, when the renormalized parameters Λ_i can be assumed to be linearly related to the bare parameters, namely, the scattering lengths g_i (see the Appendix). Emergence of this important relationship from two independent approaches and approximations strengthens the validity of the criterion for phase separation.

For the parameter values where both the zero and the π modes coexist, π-mode frequencies are smaller than the zero-mode frequencies. Figure 1 shows the values of Λ_a, Λ_b where the tunneling is governed by the zero mode and the π mode. For $\Lambda_b > 0$, the regime where the π modes exist is small but finite. However, by tuning Λ_b to negative values, the π modes that have not been seen in earlier studies can be observed. Variation with the parameter R, the tunneling ratio for the two species, leads to similar results, with the parameter space for the existence of π mode increasing slightly with R. The unshaded regime corresponds to MQST phase.

V. TUNNELING DYNAMICS WITH $\Lambda_a=\Lambda_b$

We now describe the numerical solution of the tunneling equations, solved using the standard numerical (sixth order)

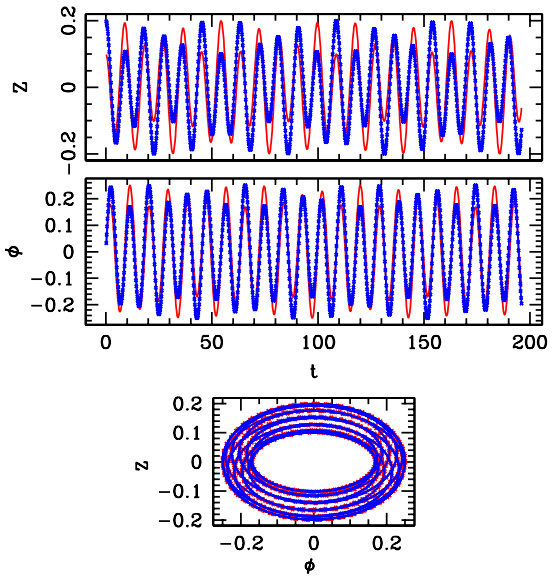

FIG. 2. (Color online) Time series for Z_l (top), ϕ_l (middle), and phase portrait for $\Lambda=0.6$ with initial conditions shown in the figure. The thin line (red) and the line with crosses (blue) correspond to the a and the b species, respectively.

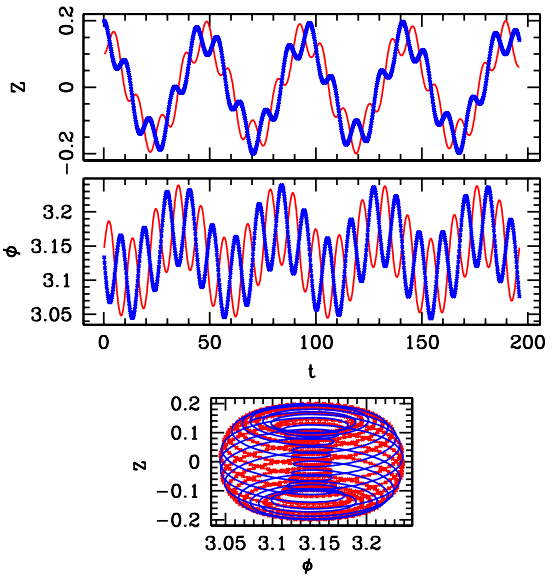

FIG. 3. (Color online) Same parameters as Fig. 2; the only exception being that $\phi_l(t=0)=\pi$ here.

Runge-Kutta method. For small population imbalance, we confirm the dynamics predicted by the fixed points as discussed above. However, numerical solutions also illustrate nonlinear modes not described by the fixed-point analysis. The fact that new features continue to exist in the nonlinear regime assures their robustness.

In our numerics, we set $\Lambda_{ab}=2.13\Lambda$ and study the dynamics for different values of Λ. These conditions can be achieved by first tuning the g_b via a Feshbach resonance so that $\Lambda_a=\Lambda_b$. The variation of Λ corresponds to varying the number of atoms in the double-well trap. As already mentioned, K can be eliminated by using $t\to Kt$ and $\Lambda\to\Lambda/K$. The dynamics is governed by Λ and the initial conditions $Z_a(0)$, $Z_b(0)$, $\phi_a(0)$, and $\phi_b(0)$.

As we discuss below, tunneling solutions belong to three broad categories:

(i) zero-phase mode, characterized by $\langle\phi_l\rangle=0$;

(ii) π-phase mode characterized by $\langle\phi_l\rangle=\pi$;

(iii) "running-phase mode" characterized by $\langle\phi_l\rangle$ proportional to t, where $\langle A\rangle$ represents the time average of A. In the single species case, $\langle\phi_l\rangle=0$ also corresponds to $\langle Z_l\rangle=0$. However, as we discuss below, in a binary mixture, we can have $\langle\phi_l\rangle=0$ but $\langle Z_l\rangle\neq 0$. This gives rise to a broken-symmetry MQST phase in zero modes as well.

A. Zero modes

For $\Lambda<\Lambda_c^0\approx 1.77$, $\phi_a(0)=\phi_b(0)=0$ and $|Z_l(0)|\ll 1$, both species execute small amplitude oscillations (such as oscillations of a nonrigid pendulum) with $\langle Z_l(t)\rangle=0$ and $\langle\phi_l(t)\rangle=0$ as shown in Fig. 2. Such modes exhibit quasiperiodic dynamics characterized by superposition of sinusoidal modes with two competing frequencies. As $Z_l(0)$ increases, we see large amplitude nonsinusoidal oscillations. Therefore, in spite of the repulsive interaction between the two condensates, the two species execute a coherent oscillatory dynamics as expected from the zero-mode fixed-point analysis described earlier in Sec. III.

B. π modes

If the dynamics is initiated with $\phi_a(t=0)=\phi_b(t=0)=\pi$, both species oscillate in π mode provided $\Lambda<\Lambda_c^0\approx 0.67$ and initial population imbalance is small $[|Z_l(0)|\ll 1]$. Analogous to the zero mode, the dynamics in the π mode is in general quasiperiodic. As seen in the Fig. 3, the motion is in phase with the slow mode and out of phase with the other. Comparison to the zero- and the π-mode oscillations show that species move more sluggishly in π mode compared to the zero mode as the zero-mode frequencies are larger than those of the π mode.

C. Symmetry breaking and phase separation: MQST in zero mode

Beyond a critical value of Λ, the system enters the symmetry-breaking MQST phase, as predicted by the fixed-point analysis earlier. One of the novel aspects of the binary mixture is the existence of zero-mode MQST accompanied by phase separation of the two species. Even with the initial conditions corresponding to abundance of both species in the same well, the two components localize in the two different wells. In this case, transition to MQST is accompanied by phase separation: although the two species overlap for some time, the $\langle Z_a(t)\rangle$ and the $\langle Z_b(t)\rangle$ have opposite signs. In the symmetric case, the condition for phase separation (10) reduces to $\Lambda_{ab}\geq\Lambda$.

D. Symmetry restoring and phase separation: Swapping mode

As Λ increases further, the system exhibits "swapping modes" where the two species swap places between the two

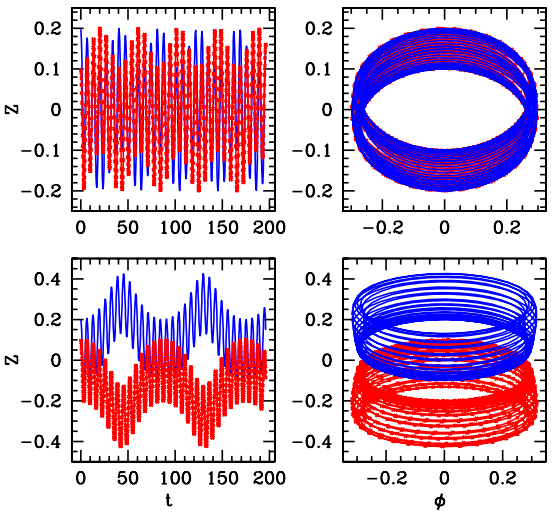

FIG. 4. (Color online) Transition from Josephson oscillations (top with $\Lambda=1.6$) to MQST with phase separation (bottom, with $\Lambda=1.8$), obtained by varying Λ. The left and right plots show the time series and phase portraits, respectively.

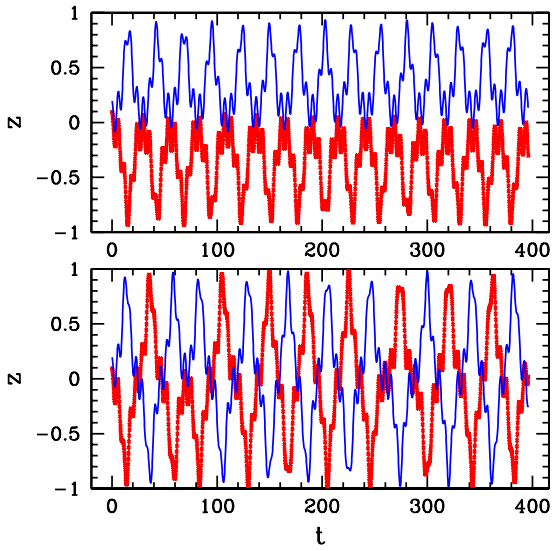

FIG. 5. (Color online) Symmetry restoring transition by varying Λ where the upper panel with $\Lambda=2.3$ shows MQST phase with phase separation while the lower panel with $\Lambda=2.5$ shows phase separation due to swapping mode.

wells but remain phase separated as shown in Fig. 4. As seen in the figure (at $t=0$), the dynamics is initiated with positive population imbalance of both species. However, the resulting dynamics corresponds to back and forth motion where the two species swap places between the two wells. In contrast to MQST, the swapping dynamics restores the symmetry of the tunneling solution in the double well. However, the two species remain mostly phase separated, *avoiding each other by swapping*.

In other words, the swapping phase is characterized by $\langle Z_a(t)\rangle = < Z_b(t) = 0$, but $< Z_a(t) Z_b(t) \neq \langle 0\rangle$. That is, at a given instant of time, the two species are more likely to be found in separate wells. Thus in the swapping mode, the two species oscillate back and forth between the two wells and still manage to avoid each other. The swapping is found to occur in the nonlinear zero mode as well as in the running mode. Furthermore, a transition from MQST to swapping phase can be achieved either by varying Λ (Fig. 5) or by varying the initial conditions (Fig. 6).

E. Symmetry breaking in π modes: Coexistence phase

For $\Lambda < \Lambda_c \approx 0.67$, $\phi_a(t=0) = \phi_b(t=0) = \pi$ and $|Z_l(t=0)| \ll 1$, both species execute small amplitude oscillations with $\langle Z_l(t)\rangle = 0 >$ and $\langle \phi_l(t)\rangle = \pi$, as shown in Fig. 7. Such modes are characterized by superposition of sinusoidal modes with two competing frequencies and the resulting dynamics is in general quasiperiodic. As expected from the fixed-point analysis, the two species with both interspecies and intraspecies repulsive interactions can self-trap in the same well. That is, we have MQST where the species coexist in the same potential well, in spite of repulsive interaction among them.

F. Swapping in π modes

As illustrated in Fig. 8, within the π-mode phase, if the dynamics of the two species is initiated in separate wells, that is, $Z_a(t=0)$ and $Z_b(t=0)$ have opposite signs, the MQST phase can be destroyed when the initial population imbalance increases beyond a critical value. The tunneling solutions become symmetric as MQST is replaced by swapping modes. In this case the swapping can be viewed as the two species "chasing" each other.

It should be noted that the swapping dynamics in the zero and the π modes is very similar. However, swapping in the zero mode corresponds to two species avoiding each other while swapping in the π mode corresponds to one component chasing the other. This is because in the zero mode, species prefer residing in the separate wells while in the π

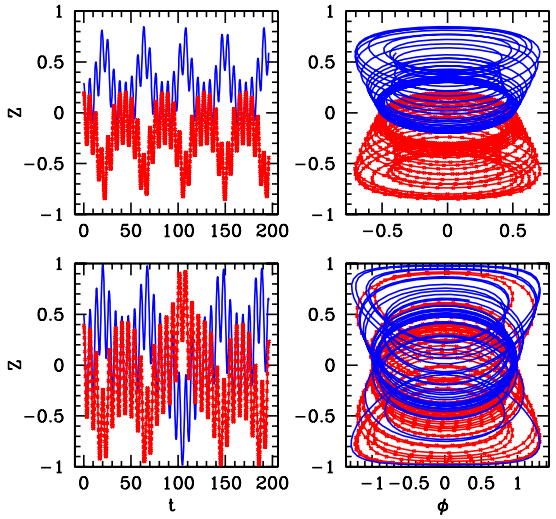

FIG. 6. (Color online) Symmetry restoring transition obtained by changing initial conditions $[Z_l(t=0)]$ slightly for fixed $\Lambda=2$. Figure shows the time series as well as the phase portraits of two species shown, respectively, with a line (blue) and line with crosses (red).

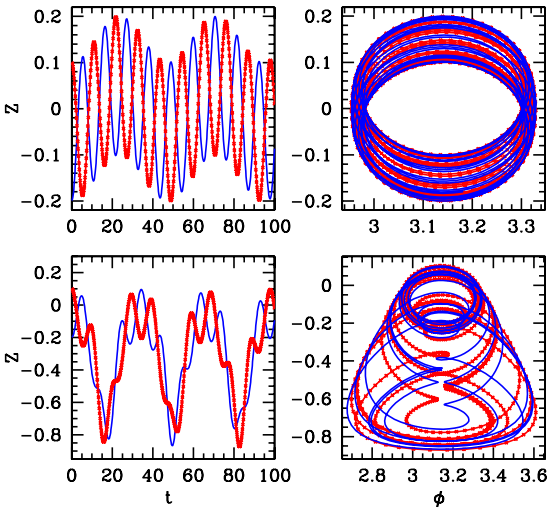

FIG. 7. (Color online) Transition to MQST in π modes. $\Lambda=0.6$ (top) and $\Lambda=0.8$ (bottom) describe, respectively, the small amplitude π-mode oscillations and MQST in π mode. The two species are, respectively, shown with a line (blue) and a line with crosses (red).

mode, they like to stay in the same well. This unique type of coherence between the two different species is one of the most fascinating aspects of the binary mixture dynamics in double-well potential.

VI. EXPERIMENTAL REALIZATION

The effects described in this paper should be realizable for condensate mixtures that already exist in the laboratory. One example in particular is a mixture of ^{85}Rb and ^{87}Rb atoms

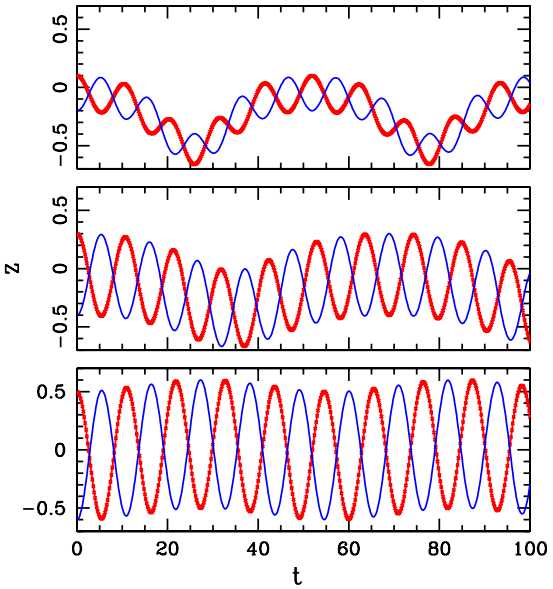

FIG. 8. (Color online) Transition from broken symmetry (MQST in π modes) to symmetric configurations, obtained by changing the initial population imbalance, with fixed $\Lambda=0.7$. The three plots correspond to three different initial conditions $[Z(0)]$ which can be read from the plot at $t=0$.

that has been created in several recent experiments at JILA [7,12]. This system is relevant to the analysis in this paper because the scattering length, a_{85-85}, that characterizes the interaction between ^{85}Rb atoms is tunable by an external magnetic field via a Feshbach resonance centered at approximately 155 [13]. Additionally, the interspecies scattering length, a_{85-87}, is also tunable with two Feshbach resonances (for a $|2,-2\rangle_{85}/|1,-1\rangle_{87}$ collision) located at approximately $B=267$ G and $B=356$ G.

In the most recent experiment [12], a ^{85}Rb/^{87}Rb BEC mixture was produced by trapping a thermal-gas sample of the mixture and performing evaporative cooling on the ^{87}Rb which sympathetically cools the ^{85}Rb. The cold gas mixture is then transferred to an optical trap that provides tight confinement transverse to the trapping beam and loose confinement along the beam. If an additional pair of beams were applied along this direction as was done in the Albiez experiment [5], it would create a setup to which the analysis in this paper would apply.

VII. SUMMARY

Existence of a variety of BEC species with tunable inter- and intraspecies scattering lengths makes BEC mixtures one of the most attractive candidates for exploring novel phenomena involving quantum coherence and nonlinearity. Our analysis, based on the two-mode GP equation for the two interacting species of BEC in a double-well trap unveils a variety of phenomena describing broken symmetry as well as subsequent restoration of symmetry, as we change the parameters or the initial conditions. Such coherence is found to exist over a broad range of parameters, establishing the robustness of the effects.

To make direct comparison with experiments, we need to solve the coupled GP equations to obtain various parameters of the effective coupled pendulum system in terms of the microscopic parameters of the system and work in this direction is in progress. Furthermore, by quantizing the Hamiltonian (coupled pendulum or the spin Hamiltonian), we hope to study quantum dynamics of number fluctuations that may code the emergence of new quantum phases in the system.

ACKNOWLEDGMENTS

R. B. thanks the council of Scientific and Industrial Research, India for financial support.

APPENDIX: TWO-MODE EQUATION PARAMETERS

We follow the improved two-mode approximation [9] where the localized spatial modes $\chi^x_{1(2)}$ in each well of the double well are constructed by using $\pm$ combinations of the symmetric (χ_+) and the antisymmetric (χ_-) functions, $\chi^x_{1,2}=\frac{\chi^x_+\pm\chi^x_-}{\sqrt{2}}$. Here $\chi^x_\pm(x)=\pm\chi^x_\pm(-x)$ are the solutions of the time-independent coupled GPE equations

$$\mu^{(a)}_j\chi^{(a)}_j(x)=-\frac{\hbar^2}{2m_a}\frac{\partial^2\chi^{(a)}_j}{\partial x^2}+V_a(x)\chi^{(a)}_j+g_aN_a|\chi^{(a)}_j|^2\chi^{(a)}_j+g_{ab}N_b|\chi^{(b)}_j|^2\chi^{(a)}_j, \quad \text{(A1)}$$

$$\mu_j^{(b)}\chi_j^{(b)}(x) = -\frac{\hbar^2}{2m_b}\frac{\partial^2\chi_j^{(b)}}{\partial x^2} + V_b(x)\chi_j^{(b)} + g_b N_b|\chi_j^{(b)}|^2\chi_j^{(b)} + g_{ba}N_a|\chi_j^{(a)}|^2\chi_j^{(b)}, \quad \text{(A2)}$$

where $j=\pm$ and labels the ground and the first-excited state of the system.

Thus $\chi_1^x(\chi_2^x)$ is localized in the left (right) well of the double-well potential. We define $\bar{g}_x=g_xN/\hbar(x=a,b,ab)$ and follow the methodology described in the earlier studies for the single-component problem [9] obtaining the following parameters that determine the tunneling dynamics for the binary mixture:

$$\Lambda_a(b) = \bar{g}_{a(b)}\int (2(\chi_+^{a(b)}\chi_-^{a(b)})^2 - 1/8\ [(\chi_-^{a(b)})^2 - (\chi_+^{a(b)})^2]^2\})dr,$$

$$\Lambda_{ab} = 2\bar{g}_{ab}\int (\chi_+^a\chi_-^a\chi_+^b\chi_-^b)dr,$$

$$\gamma_{a(b)}^{\pm} = \bar{g}_{a(b)}\int [(\chi_\pm^{a(b)})^4]dr,$$

$$\bar{\gamma}_{a(b)} = \bar{g}_{a(b)}\int [(\chi_+^{a(b)})^2(\chi_-^{a(b)})^2]dr,$$

$$\Delta\gamma_{a(b)} = \gamma_{a(b)}^- - \gamma_{a(b)}^+,$$

$$\Delta\gamma_{ab} = \bar{g}_{ab}\int [(\chi_-^a\chi_-^b)^2 - (\chi_+^a\chi_+^b)^2]dr,$$

$$\Delta\bar{\gamma}_{ab} = \bar{g}_{ab}\int [(\chi_-^a\chi_+^b)^2 - (\chi_+^a\chi_-^b)^2]dr,$$

$$K_a = [\Delta E_a - f_a\Delta\gamma_a - f_bD_{ab}]/\hbar,$$

$$K_b = [\Delta E_b - f_b\Delta\gamma_b - f_aD_{ab}]/\hbar,$$

$$C_a = (\gamma_+^a + \gamma_-^a - 2\bar{\gamma}_a)/2\hbar,$$

$$C_b = (\gamma_+^b + \gamma_-^b - 2\bar{\gamma}_b)/2\hbar,$$

$$D_{ab} = (\Delta\gamma_{ab} - \Delta\bar{\gamma}_{ab})/2\hbar.$$

Here $\Delta E_x=\mu_x^+-\mu_x^-$ represents the difference in the chemical potential between the (symmetric) ground and the (antisymmetric) first-excited state of the coupled time-independent GPE equations. It should be noted that within the two-mode ansatz, the tunneling Eqs. (5)–(8) with dressed parameters as given above are exact.

The above equations signify the importance of spatial modes in determining the temporal dynamics of the two species in the double-well potential. The Λ_x describes the renormalization of the bare coupling parameters g_x due to averaging over the spatial degrees of freedom. As expected, the renormalized couplings $\Lambda_{a(b)}$ depend upon the corresponding spatial mode $\chi_{a(b)}$ while the coupling Λ_{ab} is determined by the overlap integral between the two species. The tunneling parameters K_x that depend only on ΔE for noninteracting systems are appropriately affected by the interaction between the species.

[1] M. H. Anderson J. R. Ensher, M. R. Matthews, C. E. Wieman, and E. A. Cornell, Science **269**, 198 (1995); K. B. Davis, M. O. Mewes, M. R. Andrews, N. J. van Druten, D. S. Durfee, D. M. Kurn, and W. Ketterle, Phys. Rev. Lett. **75**, 3969 (1995); C. C. Bradley, C. A. Sackett, J. J. Tollett, and R. G. Hulet, *ibid.* **75**, 1687 (1995).

[2] G. Thalhammer, G. Barontini, L. De Sarlo, J. Catani, F. Minardi, and M. Inguscio, Phys. Rev. Lett. **100**, 210402 (2008).

[3] A. Smerzi, S. Fantoni, S. Giovanazzi, and S. R. Shenoy, Phys. Rev. Lett. **79**, 4950 (1997); S. Raghavan, A. Smerzi, S. Fantoni, and S. R. Shenoy, Phys. Rev. A **59**, 620 (1999).

[4] G. J. Milburn, J. Corney, E. M. Wright, and D. F. Walls, Phys. Rev. A **55**, 4318 (1997).

[5] M. Albiez, R. Gati, J. Folling, S. Hunsmann, M. Cristiani, and M. K. Oberthaler, Phys. Rev. Lett. **95**, 010402 (2005); see also, R. Gati, M. Albiez, J. Foelling, and B. Hemmerli, Appl. Phys. B **82**, 207 (2006).

[6] S. Papp, Ph.D thesis, University of Colorado, 2007.

[7] S. B. Papp and C. E. Wieman, Phys. Rev. Lett. **97**, 180404 (2006).

[8] Tin-Lun Ho and V. B. Shenoy, Phys. Rev. Lett. **77**, 3276 (1996); H. Pu and N. P. Bigelow, *ibid.* **80**, 1130 (1998); D. Schumayer and B. Apagyi, Phys. Rev. A **69**, 043620 (2004); D. Schumayer and B. Apagyi, Eur. Phys. J. B **45**, 55 (2004).

[9] D. Ananikian and T. Bergeman, Phys. Rev. A **74**, 039905(E) (2006).

[10] J. Chen, Y.-Q. Guo, H.-J. Cao, and H.-S. Song, Phys. Lett. A **360**, 429 (2007).

[11] S. Ashhab and C. Lobo, Phys. Rev. A **66**, 013609 (2002).

[12] S. B. Papp, J. M. Pino, and C. E. Wieman, Phys. Rev. Lett. **101**, 040402 (2008).

[13] J. P. Burke and J. L. Bohn, Phys. Rev. A **59**, 1303 (1999); J. P. Burke, J. L. Bohn, B. D. Esry, and C. H. Greene, Phys. Rev. Lett. **80**, 2097 (1998).